AIAA JOURNAL
Vol. 36, No. 8, August 1998

Space-Based-Laser Wavelength Selection for Existing Beam Control Technology Levels

Frederic H. White*
Science Applications International Corporation, Moorpark, California 93021-3021

Although conventional wisdom suggests that, for space-based-laser missions, the shortest wavelength is most desirable, this is not always the case. We show, for reasonable values of wave front error and jitter (with the majority of the wave front error in the high spatial frequencies), that deuterium fluoride (DF) is the preferred choice over shorter, e.g., hydrogen fluoride, wavelengths. Here we have considered only free-space propagation; atmospheric effects, which give further advantage to DF, are not considered.

Introduction

THIS paper is a companion to those of Acebal.[1,2] It is an extension of a paper presented by the author at the AIAA 28th Plasmadynamics and Lasers Conference.[3] We have chosen to restrict our wavelength-selection consideration to issues of beam control technology; Acebal[1,2] extends his considerations to broader laser-related issues.

To limit the problem, we consider that several key variables, e.g., laser power, telescope diameter, etc., are constant. We take as our performance variable the time-averaged, on-axis peak irradiance at the target and observe its functional dependence on beam control performance and wavelength. We characterize the beam control performance in terms of the residual beam jitter and wave front error.

We assume that these beam control performance variables have an impact on the phase of the laser beam, which scales with wavelength in a geometric-optics fashion. We find the wavelength that optimizes the target's time-averaged, on-axis peak irradiance for various levels of residual jitter and wave front error. We consider three versions of the space-based-laser technology—a deuterium fluoride (DF) laser, a hydrogen fluoride (HF) laser, and an HF overtone laser—and define a two-dimensional map of jitter and wave front error, with regions specified where each of these three laser types is the choice for the highest value of the target's time-averaged, far-field peak irradiance.

This paper is organized into three parts. The first part is a discussion of our assumptions for this analysis. The second part is the derivation of our wavelength-scaling equations. The third is a parametric presentation of the results of the wavelength-optimization analysis.

Analysis Assumptions

We assume that the degradation of the far-field peak irradiance can be attributed to three sources: residual beam jitter, residual wave front error containing low spatial frequencies, and residual wave front error containing high spatial frequencies. We designate these as residual because we assume that they are the errors remaining on the laser wave front after correction by both a fast steering mirror and a deformable mirror. We assume that these sources are independent of the laser wavelength, for the following reasons.

1) The uncorrected sources of beam jitter and wave front error are independent of wavelength. The jitter arises from vibrations in the system, which do not depend on laser wavelength. The wave front error (in microns) is determined by the static and time-varying mirror misfigures, which do not depend on laser wavelength.

2) The error rejection of the beam control system is independent of wavelength. Although the signal-to-noise ratio of the measured wave front is generically better at shorter wavelengths, it will be made high at any wavelength because there is ample laser power for the measurement. In a well-executed design, noise in the wave front measurement has become a small part of the residual wave front error. What dominates both the residual wave front error and the residual jitter is the unrejected error remaining after the control system had operated on the wave front out of the laser. The frequency response of the beam control system is determined by the mechanical properties of the fast steering mirror and the deformable mirror, in conjunction with the time it takes the control computer to calculate its correction. These are independent of laser wavelength. Consequently, the error rejection function will be independent of laser wavelength. Because the residual jitter and wave front error are each sums of products of an uncorrected set of sources and the corresponding error rejection functions and because both sources and functions are independent of laser wavelength, the sums of the products, i.e., residual jitter and wave front error, are also independent of laser wavelength.

Derivation of Wavelength-Scaling Equations

Approach

We will start with the far field of an ideal beam and show how wave front error and jitter can be modeled as degradations to that ideal beam. We begin with the Strehl ratio. Next we add a term for beam jitter. We modify our expressions to differentiate between low spatial frequencies and high spatial frequencies. Finally, we solve for the optimum wavelength.

Diffraction-Limited Performance

The theoretical value of far-field peak irradiance I_{th} for a uniformly illuminated circular aperture has been calculated by Holmes and Avizonis[4,5]:

$$I_{\text{th}} = \frac{\pi D^2 [PT]}{(2z\lambda)^2} \tag{1}$$

where $[PT]$ is the power leaving the aperture, D is the aperture diameter, z is the distance to the far-field target, and λ is the wavelength. The term P is the laser power, and T is a transmission factor that accounts for beam train losses. This functional form, with the wavelength raised to the -2 power, shows the potentially significant advantage a shorter wavelength can have.

Strehl Ratio

The Strehl intensity has been defined by Born and Wolf.[6] They start by expanding the phase function

$$\exp(ik\delta_p) = 1 + ik\delta_p + \tfrac{1}{2}(ik\delta_p)^2 + \cdots \tag{2}$$

with $k = 2\pi/\lambda$. The Strehl intensity at a focus point p is given as

$$i(p) \sim \left|1 + \overline{\delta_p} - \tfrac{1}{2}k^2\overline{\delta_p^2}\right|^2 \sim 1 - (2\pi/\lambda)^2\left[\overline{\delta_p^2} - (\overline{\delta_p})^2\right]$$

$$\sim 1 - (2\pi/\lambda)^2(\delta_{\text{rms}})^2 \tag{3}$$

Presented as Paper 97-2421 at the AIAA 28th Plasmadynamics and Lasers Conference, Atlanta, GA, June 23–25, 1997; revision received April 8, 1998; accepted for publication April 10, 1998.

*Principal Scientist, 13454 Canyonwood Court.

where the mean square phase is defined by an area integral

$$(\delta_{\rm rms})^2 = \frac{\int_0^1 \int_0^{2\pi} (\delta_P - \overline{\delta_P})^2 \rho \, {\rm d}\rho \, {\rm d}\delta}{\int_0^1 \int_0^{2\pi} \rho \, {\rm d}\rho \, {\rm d}\delta} = \overline{\delta_P^2} - (\overline{\delta_P})^2 \tag{4}$$

This Strehl intensity multiplies the ideal far-field irradiance of Eq. (1). Thus, it is also called the Strehl ratio, which is the ratio of the degraded far-field peak irradiance to that of the ideal far-field peak irradiance.

Generalized Far-Field Peak Irradiance

Holmes and Avizonis[5] have generalized the degraded time-averaged far-field peak irradiance:

$$I_{\rm ff} = I_{\rm th} \frac{\exp\left[-(2\pi\delta_{\rm rms}/\lambda)^2\right]}{1 + (1.67\sigma_J D/\lambda)^2} \tag{5}$$

where the numerator is a generalized Strehl ratio and the denominator is a term that accounts for the effects of beam jitter: σ_J is the two-axis, line-of-sight rms value of the beam jitter.

Degradation by Beam Jitter: Derivation

We will follow the approach used by Holmes and Avizonis[5] to derive Eq. (5) and obtain identical results, except for a numeric constant. Beam jitter causes the far-field spot to wander in the vicinity of the target. Typically, for transverse coordinates x and y, beam jitter (an angle measured in radians) in either coordinate is written as a zero-mean Gaussian random variable with standard deviations σ_x and σ_y for each respective coordinate. Assuming the jitter is approximately equal in x and y, the two-axis, line-of-sight rms jitter σ_J can be defined as

$$\sigma_J = \sqrt{\sigma_x^2 + \sigma_y^2} \tag{6}$$

where the radial line-of-sight jitter has a Rayleigh probability density function given by

$$p_R(\rho) = \int_0^\infty \frac{1}{\sigma_x^2} \rho \exp\left(-\frac{\rho^2}{2\sigma_x^2}\right) {\rm d}\rho = \int_0^\infty \frac{2}{\sigma_J^2} \rho \exp\left(-\frac{\rho^2}{\sigma_J^2}\right) {\rm d}\rho \tag{7}$$

Following Holmes and Avizonis,[5] we take the far-field distribution to be an Airy disk, given by

$$I_f(\rho) = \left\{\frac{2J_1[\pi(\rho/\rho_o)]}{\pi(\rho/\rho_o)}\right\}^2, \qquad \rho_o = \frac{\lambda}{D} \tag{8}$$

Note that the function J_1 is a Bessel function of the first kind and order one. The time-averaged, far-field peak irradiance of this ideal beam can be found (assuming ergodicity) by integrating over the probability density function:

$$I_{fJ}(\sigma_J) = \int_0^\infty \left\{\frac{2J_1[\pi(\rho/\rho_o)]}{\pi(\rho/\rho_o)}\right\}^2 \frac{2}{\sigma_J^2} \rho \exp\left(-\frac{\rho^2}{\sigma_J^2}\right) {\rm d}\rho \tag{9}$$

A plot of this function is shown in Fig. 1 as the solid line. Using the expression of Holmes and Avizonis,[5] their form of the far-field, jitter-degraded irradiance is

$$I_{fJH}(\sigma_J) = \frac{1}{1 + (1.67\sigma_J D/\lambda)^2} \tag{10}$$

which is shown in Fig. 1 by the dashed line. Adjusting the constant in this equation from 1.67 to $\pi/2 = 1.571$ gives a least-squares fit through the 20 data points calculated. We write

$$I_{fJ}(\sigma_J) = \frac{1}{1 + \{[(\pi/2)\sigma_J D]/\lambda\}^2} \tag{11}$$

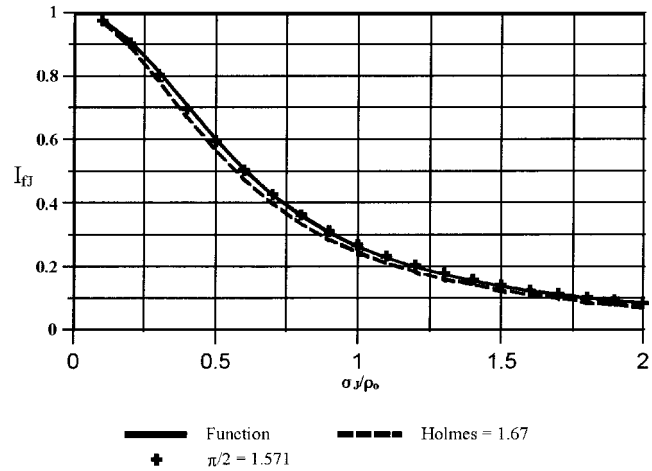

Fig. 1 Jitter-degraded, far-field peak irradiance I_{fJ} vs jitter level σ_J/ρ_o.

This equation is shown as the crosses in Fig. 1. This is the functional form we choose to retain, a slight modification to the results of Holmes and Avizonis[5] in our Eq. (5). We now modify our form of the far-field peak irradiance:

$$I_{\rm ff} = \frac{P}{z^2} T \frac{\exp\left[-(2\pi\delta_{\rm rms}/\lambda)^2\right]}{\left\{\pi\left[(2\lambda/\pi D)^2 + \sigma_J^2\right]\right\}} \tag{12}$$

Combining this with Eq. (1) and rearranging, we write

$$I_{\rm ff} = I_{\rm th} \frac{\exp\left[-(2\pi\delta_{\rm rms}/\lambda)^2\right]}{1 + \{[(\pi/2)\sigma_J D]/\lambda\}^2} \tag{13}$$

We define a line-of-sight diffraction spot size

$$\sigma_{D\rho} = 2\lambda/\pi D \tag{14}$$

which allows us to write

$$I_{\rm ff} = \frac{P}{z^2} T \frac{\exp\left[-(2\pi\delta_{\rm rms}/\lambda)^2\right]}{\left(\pi\left[\sigma_{D\rho}^2 + \sigma_J^2\right]\right)} \tag{15}$$

Revised Far-Field Peak Irradiance

The equations presented so far have made the assumption that the far-field spot remains approximately an Airy disk. Although this is the case for high spatial frequencies, it is not correct for low spatial frequencies, such as astigmatism. We say that the beam quality is degraded and that the far-field spot is broadened to β_L times its diffraction-limited size. We associate the Strehl-type degradation of the numerator in Eq. (15) with high spatial frequencies and write

$$I_{\rm ff} = \frac{P}{z^2} T \frac{\exp\left[-(2\pi\delta_{H\,\rm rms}/\lambda)^2\right]}{\pi\left[(\beta_L\sigma_{D\rho})^2 + \sigma_J^2\right]} \tag{16}$$

where the low-spatial-frequency beam quality is defined by Acebal[1]:

$$\beta_L = \sqrt{1 + \left(\frac{2\pi\delta_{L\,\rm rms}}{\lambda}\right)^2} \tag{17}$$

We have defined the preceding equations in terms of two-axis, line-of-sight beam jitter. Temporarily, recalling that the line-of-sight jitter is related to the single-axis jitter by a factor of the $\sqrt{2}$,

$$\sigma_J = \sqrt{2}\sigma_x \tag{18}$$

We also can expand the numerator of Eq. (16) and retain the first two terms:

$$I_{\text{ff}} = \frac{PT}{z^2}\frac{1}{\left[1+(2\pi\delta_{H\,\text{rms}}/\lambda)^2\right]2\pi\left[(\beta_L\sigma_{Dx})^2+\sigma_x^2\right]}$$

$$= \frac{PT/z^2}{\beta_H^2(2\pi)\left[(\beta_L\sigma_{Dx})^2+\sigma_x^2\right]} \tag{19}$$

where

$$\beta_H^2 = 1+\left(\frac{2\pi\delta_{H\,\text{rms}}}{\lambda}\right)^2 \tag{20}$$

and the single-axis diffraction spot size is

$$\sigma_{Dx} = \sqrt{2}\lambda/\pi D \tag{21}$$

Equation (19) is the form for the far-field intensity given by Acebal.[1]

Wavelength Dependency

Equation (16) can be written with its specific wavelength dependency:

$$I_{\text{ff}} = \frac{P}{z^2}T\frac{\exp\left[-(2\pi\delta_{H\,\text{rms}}/\lambda)^2\right]}{\pi\left\{\left[1+(2\pi\delta_{L\,\text{rms}}/\lambda)^2\right](2\lambda/\pi D)^2+\sigma_J^2\right\}} \tag{22}$$

We find the optimum wavelength by differentiating Eq. (22) with respect to wavelength, setting this equal to zero, and solving for the wavelength. The resulting optimum wavelength is

$$\lambda_{\text{opt}} = \pi\sqrt{\delta_{H\,\text{rms}}}\sqrt{2\delta_{H\,\text{rms}}+\sqrt{4\delta_{H\,\text{rms}}^2+16\delta_{L\,\text{rms}}^2+\sigma_J^2D^2}} \tag{23}$$

This can be written as

$$\lambda_{\text{opt}} = \pi\sqrt{2}\delta_{H\,\text{rms}}\sqrt{1+\sqrt{1+\frac{16\delta_{L\,\text{rms}}^2+\sigma_J^2D^2}{4\delta_{H\,\text{rms}}^2}}} \tag{24}$$

Analysis of Laser Wavelength Optimization

We analyzed the choice of laser wavelength parametrically, as a function of wave front error and jitter. For the residual wave front error, we chose various values of high and low spatial frequencies:

$$\frac{\delta_{L\,\text{rms}}}{\delta_{H\,\text{rms}}} = \delta_{\text{Rat}} = 0,\ \frac{1}{2},\ \frac{1}{1},\ \frac{\sqrt{2}}{1},\ \frac{2}{1},\ \frac{5}{1}$$

These wave front errors are assumed independent and therefore combine to produce the total wave front error

$$\delta_{T\,\text{rms}} = \sqrt{\delta_{H\,\text{rms}}^2+\delta_{L\,\text{rms}}^2} \tag{25}$$

Because the beam control system has a much greater error rejection at low spatial (and temporal) frequencies, the most likely residual error is one that is predominately high spatial frequencies.

We define a two-dimensional map of $\delta_{T\,\text{rms}}$ vs $\sigma_J D$. On this map we define regions for which one of the three wavelengths (a DF laser, $\lambda = 3.8$ μm; an HF laser, $\lambda = 2.7$ μm; and an HF overtone laser, $\lambda = 1.35$ μm) is the best choice. We also show as lines on the map where the three wavelengths are the exact optimum wavelength. These maps are shown in Figs. 2–7. We choose a representative set of wave front error and jitter levels. These are translated into two-axis, line-of-sight numbers for a telescope diameter of 4.0 m and shown in Table 1. We plotted these values as the crosshair in Figs. 2–7. For each of these, except for δ_{Rat} values of 2 and 5, the crosshair fell inside the DF preferred region. Consequently, we conclude that, for residual wave front errors with the low spatial frequency/high spatial frequency as high as 141%, the choice of the DF ($\lambda = 3.8$ μm) wavelength will provide superior target irradiance for the wave front error and jitter of the reference, considering only free-space propagation. Figure 7, for which the low spatial frequencies are five times the high, shows the characteristic of a system with little high spatial frequencies and also shows that the shortest wavelength is the best.

Here is a brief note on the development of the lines and regions in Figs. 2–5. The lines labeled 1.35, 2.7, and 3.8 are lines of constant wavelength in Eqs. (23) or (24), where λ_{opt} is, respectively, 1.35, 2.7, and 3.8 μm. A more convenient form for these equations may be as follows:

Table 1 Nominal wave front error and jitter values

Beam control variable	Single axis	Line of sight
Device OPD,[a] μm	0.285	0.403
Beam train OPD, μm	0.338	0.478
Total OPD, μm	0.442	0.625
1σ jitter, μrad	0.3	0.424
Jitter-diameter product, μm	1.2	1.697

[a]OPD, optical path difference.

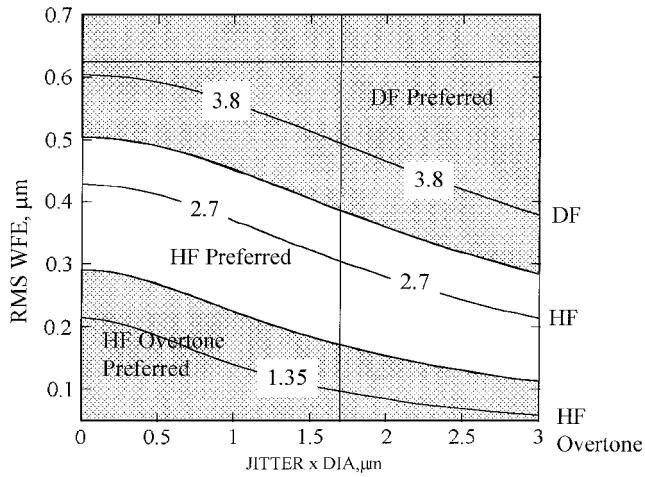

Fig. 2 Zero level of low spatial frequencies. Preferred wavelength for zero level of low spatial frequencies: $\delta_L/\delta_H = 0$.

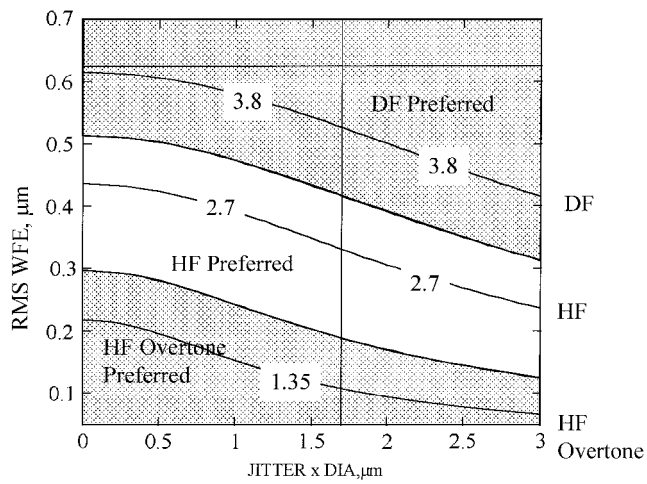

Fig. 3 Low spatial frequencies one-half of high spatial frequencies. Preferred wavelength for unequal levels of low spatial frequencies: $\delta_L/\delta_H = 1/2$.

$$D^2\cdot\sigma_J^2 = \frac{\left[-4\cdot\delta_{T\,\text{rms}}^2\cdot\pi^2\cdot\lambda_{\text{opt}}^2\cdot\left(1+\delta_{\text{Rat}}^2\right)+\lambda_{\text{opt}}^4\cdot\left(1+\delta_{\text{Rat}}^2\right)^2-16\cdot\delta_{T\,\text{rms}}^4\cdot\delta_{\text{Rat}}^2\cdot\pi^4\right]}{\left[\left(1+\delta_{\text{Rat}}^2\right)\cdot\left(\pi^4\cdot\delta_{T\,\text{rms}}^2\right)\right]} \tag{26}$$

The approach to obtaining the boundaries between the DF preferred, HF preferred, and HF overtone preferred was as follows. Equation (22) was evaluated for each of the three wavelengths for the range of values of the two independent variables: jitter × diameter, μm, and rms wave front error, μm. The boundary between DF preferred and HF preferred is where Eq. (22) has the same value for 3.8 and 2.7 μm. Similarly, the boundary between HF preferred and HF overtone preferred is where Eq. (22) has the same value for 2.7 and 1.35 μm. The boundary between two wavelength regions is described by

$$D^2 \cdot \sigma_J^2 = \frac{\left\{ \begin{array}{l} -\left[4 \cdot \exp\left[-4 \cdot \dfrac{\pi^2}{\left(1+\delta_{\text{Rat}}^2\right)} \cdot \dfrac{\delta_{T\,\text{rms}}^2}{\lambda_2^2}\right] \cdot \lambda_1^2 + 4 \cdot \exp\left[-4 \cdot \dfrac{\pi^2}{\left(1+\delta_{\text{Rat}}^2\right)} \cdot \dfrac{\delta_{T\,\text{rms}}^2}{\lambda_2^2}\right] \cdot \lambda_1^2 \cdot \delta_{\text{Rat}}^2 \right. \\ \left. + 16 \cdot \exp\left[-4 \cdot \dfrac{\pi^2}{\left(1+\delta_{\text{Rat}}^2\right)} \cdot \dfrac{\delta_{T\,\text{rms}}^2}{\lambda_2^2}\right] \cdot \pi^2 \cdot \delta_{\text{Rat}}^2 \cdot \delta_{T\,\text{rms}}^2 \right] \cdots \\ + 4 \cdot \exp\left[-4 \cdot \dfrac{\pi^2}{\left(1+\delta_{\text{Rat}}^2\right)} \cdot \dfrac{\delta_{T\,\text{rms}}^2}{\lambda_1^2}\right] \cdot \lambda 2_2 + 4 \cdot \exp\left[-4 \cdot \dfrac{\pi^2}{\left(1+\delta_{\text{Rat}}^2\right)} \cdot \dfrac{\delta_{T\,\text{rms}}^2}{\lambda_1^2}\right] \cdot \lambda_2^2 \cdot \delta_{\text{Rat}}^2 \\ + 16 \cdot \exp\left[-4 \cdot \dfrac{\pi^2}{\left(1+\delta_{\text{Rat}}^2\right)} \cdot \dfrac{\delta_{T\,\text{rms}}^2}{\lambda_1^2}\right] \cdot \pi^2 \cdot \delta_{\text{Rat}}^2 \cdot \delta_{T\,\text{rms}}^2 \end{array} \right\}}{\left\{ \begin{array}{l} -\exp\left[-4 \cdot \dfrac{\pi^2}{\left(1+\delta_{\text{Rat}}^2\right)} \cdot \dfrac{\delta_{T\,\text{rms}}^2}{\lambda_1^2}\right] \cdot \pi^2 - \exp\left[-4 \cdot \dfrac{\pi^2}{\left(1+\delta_{\text{Rat}}^2\right)} \cdot \dfrac{\delta_{T\,\text{rms}}^2}{\lambda_1^2}\right] \cdot \pi^2 \cdot \delta_{\text{Rat}}^2 \\ + \exp\left[-4 \cdot \dfrac{\pi^2}{\left(1+\delta_{\text{Rat}}^2\right)} \cdot \dfrac{\delta_{T\,\text{rms}}^2}{\lambda_2^2}\right] \cdot \pi^2 + \exp\left[-4 \cdot \dfrac{\pi^2}{\left(1+\delta_{\text{Rat}}^2\right)} \cdot \dfrac{\delta_{T\,\text{rms}}^2}{\lambda_2^2}\right] \cdot \pi^2 \cdot \delta_{\text{Rat}}^2 \end{array} \right\}} \tag{27}$$

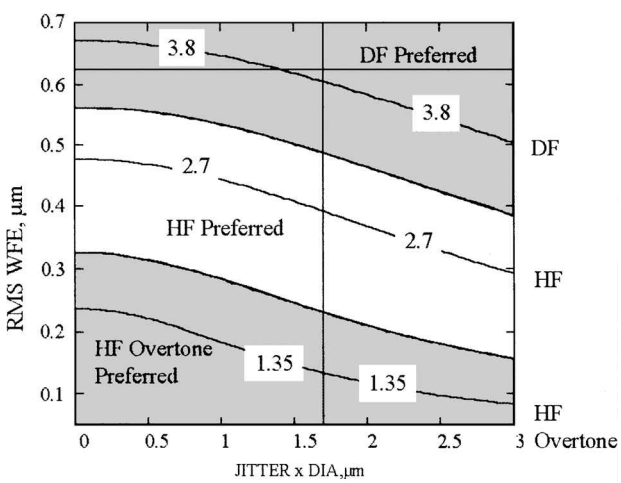

Fig. 4 Equal levels of high and low spatial frequencies. Preferred wavelength for equal levels of low spatial frequencies: $\delta_L/\delta_H = 1$.

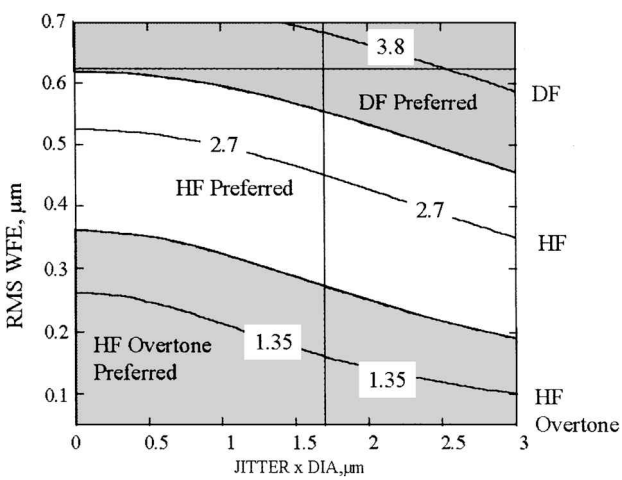

Fig. 5 Low spatial frequencies $\sqrt{2}$ times high spatial frequencies. Preferred wavelength for unequal levels of low spatial frequencies: $\delta_L/\delta_H = \sqrt{2}$.

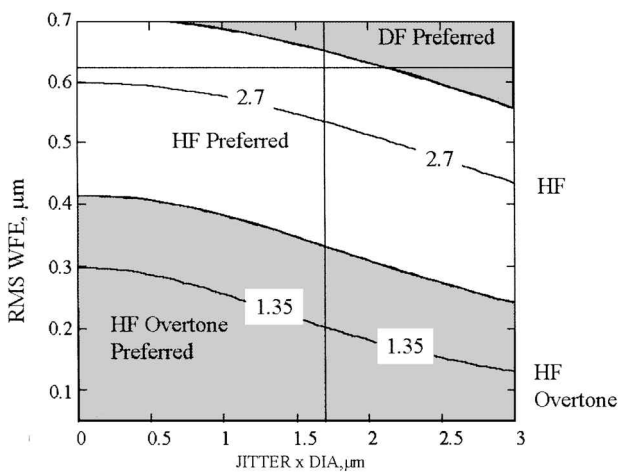

Fig. 6 Low spatial frequencies two times high spatial frequencies. Preferred wavelength for unequal levels of low spatial frequencies: $\delta_L/\delta_H = 2$.

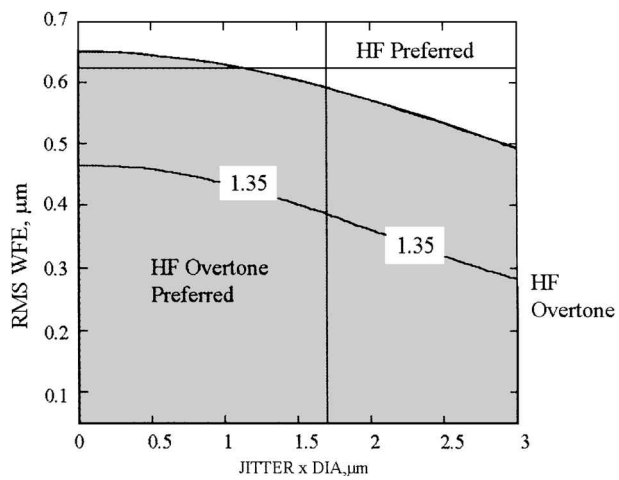

Fig. 7 Low spatial frequencies five times high spatial frequencies. Preferred wavelength for unequal levels of low spatial frequencies: $\delta_L/\delta_H = 5$.

Conclusions

We have presented an analytical formulation for the time-averaged, on-axis, far-field peak irradiance. The independent variables in our formulation are transmitter diameter, beam jitter, low-spatial-frequency wave front error, high-spatial-frequency wave front error, and wavelength. Using derivative techniques, we have found an expression for the optimal wavelength as a function of the other independent variables. We have shown, for a reasonable set of the independent variables, that a 3.8-μm wavelength of the DF laser is preferred over the shorter wavelengths of HF and HF overtone.

Acknowledgments

This work was performed under Government Contract SDIO84-92C-0008. The author wishes to acknowledge the support of the Program Manager, Lyn Skolnik, and the helpful suggestions of the reviewers.

References

[1]Acebal, R., "HF/DF System Design Issues for Space Mission Applications," AIAA Paper 97-2411, July 1997.

[2]Acebal, R., "Hydrogen Fluoride vs Deuterium Fluoride Space-Based Laser Performance Comparison," *AIAA Journal*, Vol. 36, No. 3, 1998, pp. 416–419.

[3]White, F., "SBL Wavelength Selection for Beam-Control Technology Level," AIAA Paper 97-2421, July 1997.

[4]Holmes, D. A., and Avizonis, P. V., "An Approximate Optical Systems Model," *Laser Digest*, AFWL-TR-74-100, 1974, pp. 14–28.

[5]Holmes, D. A., and Avizonis, P. V., "Approximate Optical Systems Model," *Applied Optics*, Vol. 15, No. 4, 1976, pp. 1075–1082.

[6]Born, M., and Wolf, E., *Principles of Optics*, 6th ed., Pergamon, Oxford, England, UK, 1980, pp. 463, 464.

G. Laufer
Associate Editor